# Multicolor fluorescent switches in gel systems controlled by alkoxyl chain and solvent†

**Yue Xu,[b] Pengchong Xue,*[a] Defang Xu,[a] Xiaofei Zhang,[a] Xingliang Liu,[a] Huipeng Zhou,[a] Junhui Jia,[a] Xinchun Yang,[a] Fengyong Wang[a] and Ran Lu*[a]**

***Received 7th May 2010, Accepted 6th July 2010***
**DOI: 10.1039/c0ob00091d**



Two simple molecules, **1** and **2** with D-π-A structure and alkoxyl groups, respectively, were designed and synthesized. Both compounds can gelatinize THF–water and DMSO. And compound **2** forms gel in acetone by ultrasonic stimulus. Interestingly, these gels exhibit aggregation-induced emission (AIE) during the sol–gel phase transformation. Moreover, the molecular self-assembled and photophysical properties can be controlled by the number of the alkoxyl chains and the type of the solvents. For example, **1** has an identical packing model and fluorescent colour in THF–water and DMSO gels. Contrarily, the self-assembly of molecule **2** strongly depends on the solvent. Furthermore, the gel phases of **2** formed in three solvents possess different fluorescent colours. Such as, THF–water gel emits yellow fluorescence, acetone gel has orange emission and red fluorescence appears in DMSO.

## Introduction

Recently, low-molecular-mass gelators (LMMG) have become a hot topic in materials science.[1] Various functional gel systems with potential applications in light harvesting, photoswitches, gas sensors, drug transfer and release, medical therapy, ion discerning, templated transcription and solar cell have been constructed.[2] In particular, the functionalities of π-conjugated LMMGs can be tailored by incorporating stimuli-responsive units, for example, pH sensitive, temperature-responsive and photoactive moieties. These stimuli responsive organogels, alternatively called "smart" or "intelligent" gels, usually show reversible changes in morphologies and/or physical properties in response to various external stimuli so as to result in many different kinds of switches based on these gels.[3]

If a π-conjugated gelator exhibited the aggregation-induced emission (AIE) activity,[4] the fluorescence of the gel formed by it should respond to temperature. In other words, this gel can give strong emission while nonemissive or weak fluorescent system is observed when the temperature is above $T_{gel}$ (sol–gel phase transition temperature). Thus, a smart fluorescent switch in response to temperature stimulus can be obtained. Although some π-conjugated gel systems with AIE activity have been reported by our group and others,[5] there is no investigation about the influence of the solvent and the alkoxyl chain on the characteristics of AIE and fluorescent switch in gel systems.

In this paper, we designed two π-conjugated gelators, **1** and **2** with one and two alkoxyl chains, respectively. It was found that all gels formed by **1** and **2** in different solvents exhibited the aggregation-induced emission activity. Moreover, molecular assemblies and photophysical properties could be controlled by the number of the alkoxyl chains and the type of the solvents. For example, **1** has a uniform molecular packing model and the same fluorescent color in the both gel phases. However, the self-assembly and fluorescent characteristic of **2** strongly depend on the solvent. Molecule **2** can be arranged into two kinds of the lamellar structures with different layer periods in THF–water and DMSO gels. Moreover, the gels of **2** formed in the three solvents possess different fluorescent colors. For instance, THF–water gel emits yellow fluorescence, acetone gel has orange emission and red fluorescent color appears in DMSO. Thus, the temperature-responsive and multicolor fluorescent switches could be easily obtained by adjusting the type of the solvents and the number of the alkoxyl chains.

## Results and discussion

### Photophysical properties of 1 and 2 in solution and crystal state

Because **1** and **2** are typical D-π-A type molecules (alkoxyl is an electron-pushing group and nitro is the electron-pulling unit), their UV-vis absorption and fluorescent spectra may be distinct in solvents with different polarities. As shown in Fig. 1, the maximal absorption of **1** in benzene is located at 370 nm, which shifts to 390 nm for **2** because of the stronger electron-pushing ability of the donors of **2** (two alkoxyl groups). In THF, the maximal absorption peaks shift to 372 and 391 nm for **1** and **2**, respectively, and 376 and 392 nm in $CHCl_3$. It is very clear that the absorption peaks of **1** and **2** have slight red-shifts with the increase of the solvent polarity. This indicates that the differences in the dipole moments of the Franck–Condon (FC) excited states and the ground states of **1** and **2** are quite small.[6] Unlike absorption spectra, the fluorescent spectra of **1** and **2** exhibit obvious red-shifts in polar solvents compared with those in nonpolar ones (Fig. 1b). In the case of **1**, the emission maximum at 456 nm in toluene shifts to 460 nm in benzene, 484 in THF, 493 in $CHCl_3$ and 518 nm in $CH_2Cl_2$,

[a]*State Key Laboratory of Supramolecular Structure and Materials, College of Chemistry, Jilin University, Changchun, 130012, P. R. China. E-mail: xuepengchong@jlu.edu.cn, luran@jlu.edu.cn; Tel: 86-431-88499179*
[b]*Test Science Experiment Center, Jilin University, 2699 Qianjin Street, Changchun, 130012, P. R. China*

† Electronic supplementary information (ESI) available: Frontier orbital, XRD patterns of two crystals, time-dependent UV-vis spectra of **1** in THF–water (v/v = 1/1), polarized light microscopic photos, UV–vis spectrum of **2** in acetone and temperature-dependent FL spectra. See DOI: 10.1039/c0ob00091d

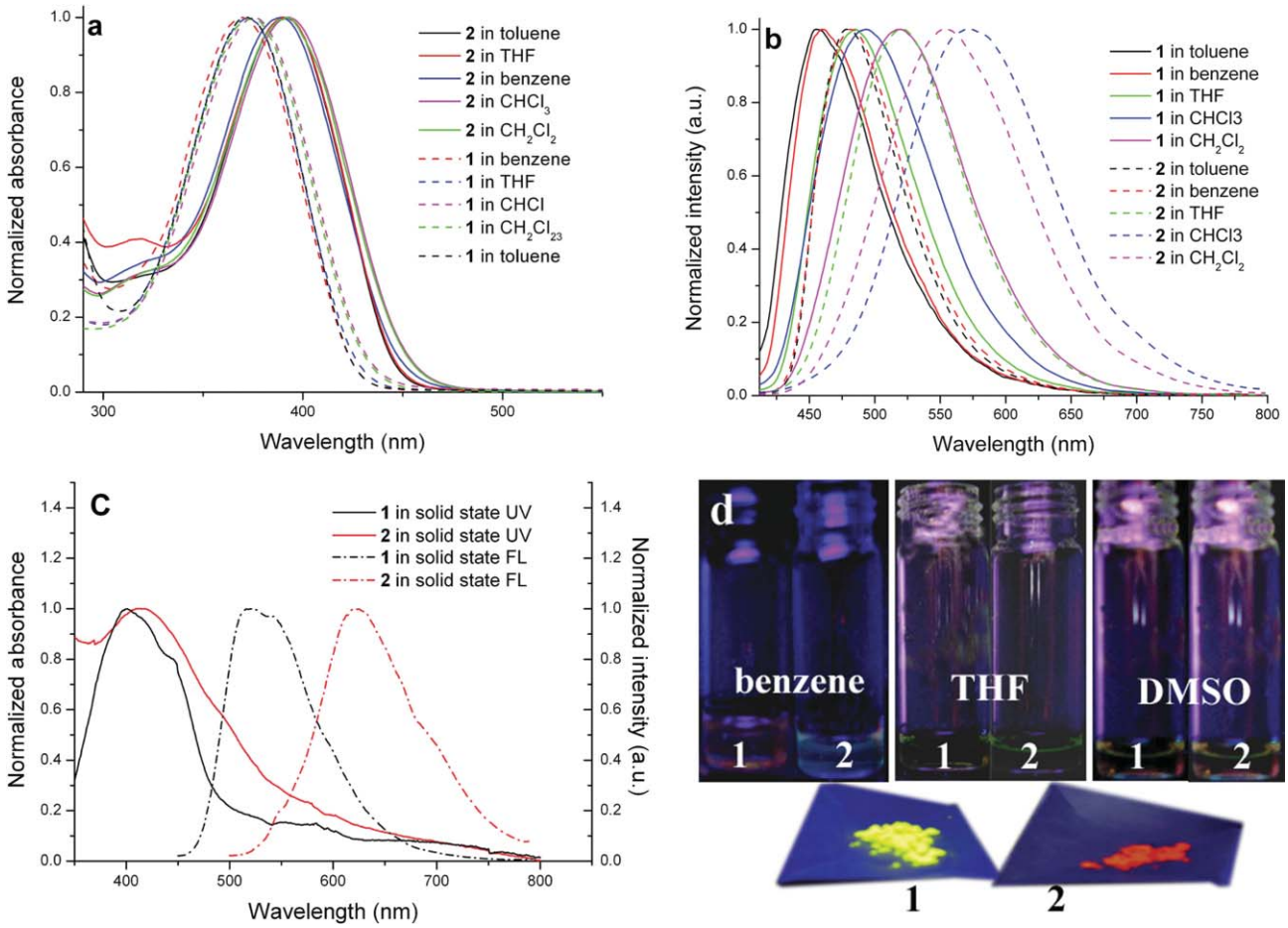


**Fig. 1** Absorption (a) and fluorescence (b) spectra of **1** and **2** in various dilute solutions, absorption and fluorescence (c) of **1** and **2** crystals and photos (d) of solutions and crystals under the irradiation of 365 nm UV light.

giving the large solvatochromic shifts of 4, 28, 37 and 62 nm, respectively. Similarly, compound **2** also shows a large red-shift of 93 nm from toluene to $CH_2Cl_2$. Therefore, the pronounced ICT characteristics of the excitation states can be deduced.[7] In addition, DFT calculation (B3LYP/6-31G) also indicates that the maximal absorption bands of **1** and **2** are assignable to the intramolecular charge transfer (ICT) transition from the HOMO mainly localized over the donor party to the LUMO mainly localized on the acceptor (nitro unit, Fig. S1†). It is worth mentioning that both **1** and **2** show weak emission in solutions. For example, the fluorescent quantum yields ($\Phi_f$) of **1** and **2** in THF are only 0.0055 and 0.0059, respectively. However, the powders of **1** and **2** can emit strong fluorescence. As seen in Fig. 1c and d, **1** shows strong yellow-green light with a maximum at 529 nm, and **2** gives intense red emission (the maximal peak at 622 nm). These data reveal that molecular aggregation can induce the emission enhancement of **1** and **2** compared with those in solution state. It has been reported that the enhanced emission of organic molecules in the crystal state has been interpreted in terms of the intra- and intermolecular effects exerted by the fluorophore aggregation. Intramolecular effects on the fluorescent enhancement can be explained by the conformational changes of the chromophores. It is supposed that the twisted conformations of chromophores in solution tend to suppress the radiative process, whereas planar ones of chromophores activate the radiation process in the crystal state. Effects on fluorescent changes by intermolecular interactions are correlated with the aggregation type, such as H- and J-aggregation. H-aggregates, where molecules are arranged in parallel with strong intermolecular interactions, prefer to induce the nonradiative deactivation process. Formation of H aggregates is characterized by the blueshift of the UV-vis absorption peak relative to isolated species. In contrast, J-aggregates, where the molecules are arranged in head-to-tail direction and the transition from the lowest couple excited state of molecule to ground state is allowed, induce a relatively high fluorescent efficiency along with an absorption bathochromic shift.[8] In this case, the existence of a cyano group is advantageous in the twisted conformation in the isolated state owing to the steric interaction between the bulky cyano unit and the neighboring hydrogen atoms,[9] which can be supported by the geometry optimization with DFT calculation, as shown in Fig. 2. Such twisted conformation always suppresses the radiation transition and then leads to weak fluorescence.[4] On the other hand, the dihedral angle between the adjacent groups can be depressed in the aggregated state, which is supported by UV-vis absorption spectra. The maximal absorption bands of **1** and **2** in crystal state locate at 401 and 418 nm (red-shifts of 31 and 28 nm compared with those in dilute benzene solutions) with the new shoulder bands at 443 and 461 nm, respectively (Fig. 1c). The peaks at 401 and 418 nm are associated with the molecular transitions with planar conformations, whose conjugation lengths

 

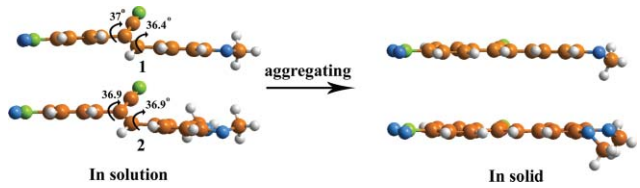


**Fig. 2** A schematic representation of planarization of **1** and **2** from twisted conformation after aggregation. Long alkoxyl chains were replaced by methoxyl groups for easy calculation and clarity.

are extended, while the bands at 443 and 461 nm are assigned to the J aggregates of **1** and **2**, respectively.[9] When the hot solution of **1** in THF–water (v/*v* = 1/1) was cooled for 1 min, the clear solution became turbid and the maximal absorption peak at 377 nm red-shifts to 387 nm, indicating J aggregation. However, at the moment system still emits weak fluorescence. After 3 min, one new peak around 450 nm appears, accompanying with rapid increase of the emission intensity. Therefore, the formation of J aggregate may be considered to be the reason for the enhanced emission.[5] In addition, further red-shifts of 42 and 43 nm of the peaks ascribing to J aggregates compared with those in planar conformation show similar π–π interaction between aromatic units, and further indicate that two alkoxyl chains do not display a more efficient π–π interaction.

Furthermore, we obtained the small- and wide-angle powder X-ray diffraction patterns of the crystals (Fig. S3†). It is very clear that two diffraction patterns show strong and sharp diffraction peaks in both low and wide angle regions. The diffraction peaks which appeared in the low-angle region illustrate the lamellar lattices with the long-range periods of 2.74 and 5.26 nm for **1** and **2**, respectively. The sharp diffraction peaks suggest the short-range ordering in wide angle region.[10] These data indicate the high ordering of the molecular stacking.

## Self-assembled properties in gel phases

**Gelation ability.** The gelation ability of **1** and **2** was checked by the standard heating-and-cooling method. From Table 1, we can find that they easily dissolve in many solvents, such as $CHCl_3$, benzene, cyclohexane, THF and ethyl acetate. Notably, **2** can form stable gel in DMSO and THF–water, while the gels of **1** in DMSO and THF–water can be easily destroyed by being shaken. In addition, **2** can gelatinize acetone by ultrasonic stimulation. So, compound **2** bearing two alkoxyl chains shows stronger gelation ability than that of **1** with one alkoxyl chain, suggesting that the alkoxyl chain has an effect on the molecular gelation ability.

**Table 1** The gelation ability of **1** and **2** in organic solvents[a]

| Solvent | 1 | 2 | Solvent | 1 | 2 |
|---|---|---|---|---|---|
| $CH_2Cl_2$ | S | S | Acetone | P | G[b] |
| $CHCl_3$ | S | S | Cyclohexanone | S | S |
| THF | S | S | Ethyl acetate | S | S |
| DMSO | G | G | Butyl acetate | S | S |
| Benzene | S | S | Cyclohexane | P | P |
| Toluene | S | S | n-Hexane | P | P |
| Ethanol | P | P | THF–water[c] | G | G |

[a] [**1**] and [**2**] = 1.0 wt/vol% (g $mL^{-1}$%); G – gel; P – precipitate; S – soluble. [b] Gel induced by ultrasonic stimulation. [c] v/*v* = 3/1.

**Microscopic observation.** The light microscopy pictures (Fig. S4†) of the gels of **1** and **2** in THF–water and DMSO illustrate that **1** prefers to form long and thick fibers, and **2** prefers to self-assemble into thinner fibers, especially in DMSO. Scanning electron microscope (SEM) was further used to study the microscopic structure of the gels. As shown in Fig. 3a and c, an extended fibrillar network was formed by numerous long and thick fibers with high aspect ratio, width of 150–500 nm and length of tens micrometres, in the THF–water and DMSO gels of **1**. On the other hand, a large amount of thinner fibers could be observed in gels of **2** (Fig. 3b and 3d). This suggests that two gelator molecules tend to self-assemble into 1-D fiber.

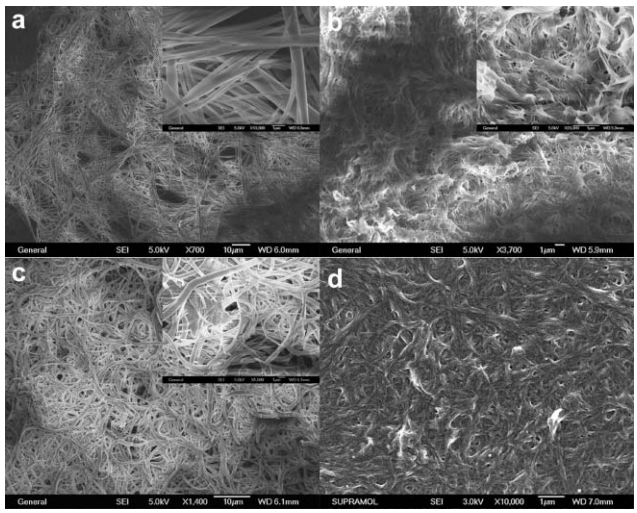


**Fig. 3** SEM images of xerogels of **1** in THF–water (v/*v* = 3/1, a), DMSO (c); **2** in THF–water (v/*v* = 3/1, b) and DMSO (d).

**Absorption spectral investigation.** The absorption spectral changes were determined to monitor the interactions between the chromophores during the gel formation. The time-dependent UV-Vis absorption spectra of compound **1** and **2** in THF–water and DMSO are shown in Fig. 4. The hot solution of **1** in THF–water (v/*v* = 3/1) gave a strong absorption maximum at 378 nm, which decreased rapidly when the sample was cooled to room temperature naturally. Its absorbance could decrease by 77% after 8 min. Moreover, a new peak at *ca.* 450 nm, appeared and became stronger and stronger with prolonging time. Similar spectral change was also observed in DMSO system of **1** and the three solvent systems of **2** (THF–water, DMSO and acetone). These spectral changes reveal that both gelators in the gel phases are also arranged into J aggregates.

**IR spectral observation.** To explore the role of cyano units and alkoxyl chains in molecular assemblies, the IR spectra of **1** and **2** in solution and gel phase were measured. As shown in Fig. 5, in dichlorobenzene solution cyano stretching appeared at 2216 and 2214 $cm^{-1}$ for **1** and **2**, respectively. In the case of xerogels, significant changes in the cyano stretching region were noticeable. The corresponding absorption peaks shifted to 2213 and 2212 $cm^{-1}$, respectively, implying the existence of cyano interactions in gel phases.[11] In addition, the antisymmetric and symmetric stretching vibration bands of $CH_2$ groups are located at 2928 and 2856 $cm^{-1}$ for **1** and **2** in dichlorobenzene solution,

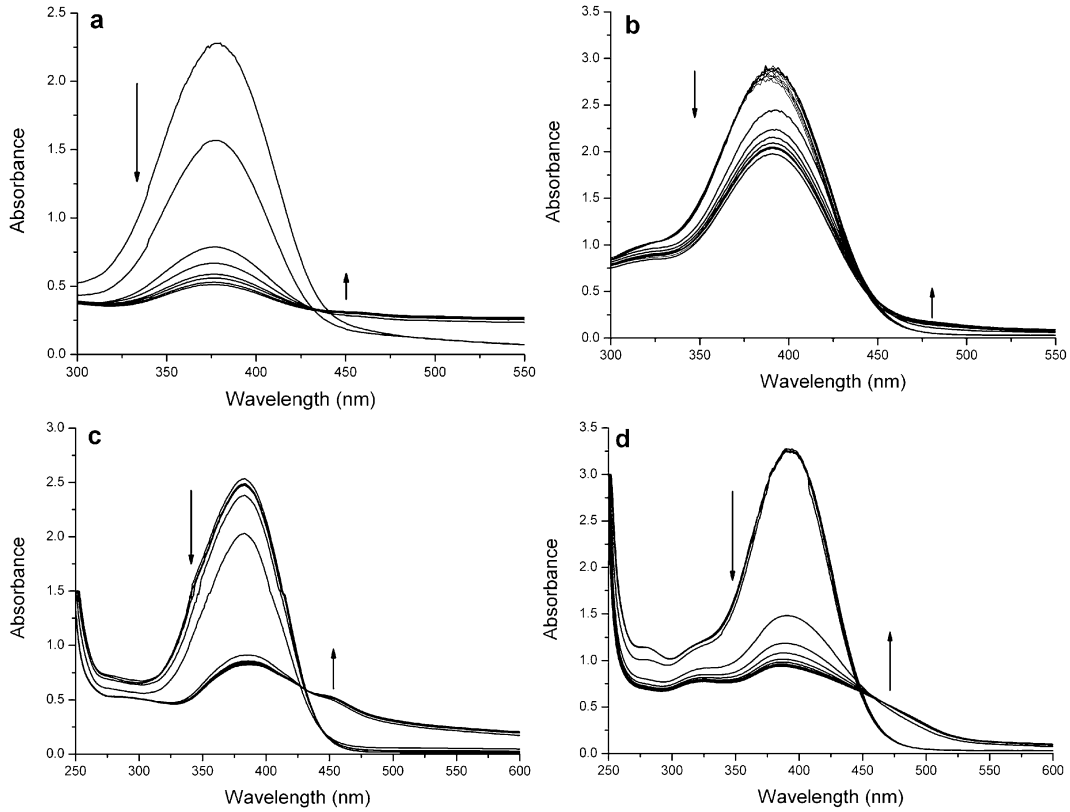


**Fig. 4** Time-dependent UV-vis spectra of **1** in THF–water (v/*v* = 3/1, a) and DMSO (c) at 0.05 wt/vol; **2** in THF–water (v/*v* = 3/1, b) and DMSO (d) at 0.1 wt/vol%. The samples in a and c were tested from 60 °C to room temperature. The samples in b and d are 100 °C to room temperature. The testing interval is 60 s.

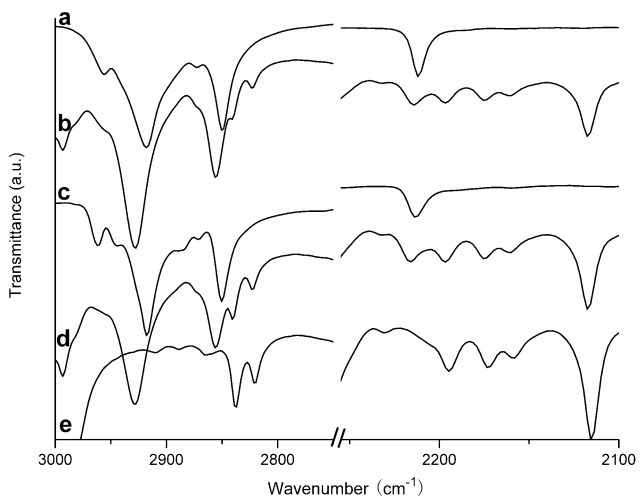


**Fig. 5** FT-IR spectra of **2** and **1** in THF–water xerogels (a and c) and in dichlorobenzene (b and d) solutions. e is IR spectrum of dichlorobenzene.

indicating the existance of the *gauche* conformations and free rotation of alkyl chain. On the other hand, in xerogels they were shifted to 2917 and 2850 $cm^{-1}$, respectively, meaning that the alkyl chains adopt all-*trans* extended conformation and their mobility is restricted after gel formation.[12] These results indicate that cyano interactions and van der Waals interactions between the alkyl chains also play an important role in the self-assembly of gelators.

**X-Ray diffraction studies.** To reveal the molecular packing of the gelators in the gel phases, the low-angle XRD patterns of xerogels of **1** and **2** obtained from THF–water and DMSO were investigated and shown in Fig. 6. It is clear that the X-ray diffraction peak locations of the xerogels of **1** are the same as those in crystal sate, which indicates that molecule **1** also adopts a lamellar packing structure with the domain spacing evaluated to be 2.74 nm in two solvent gel systems. The slight difference between the two solvent patterns is that the strengths of diffraction

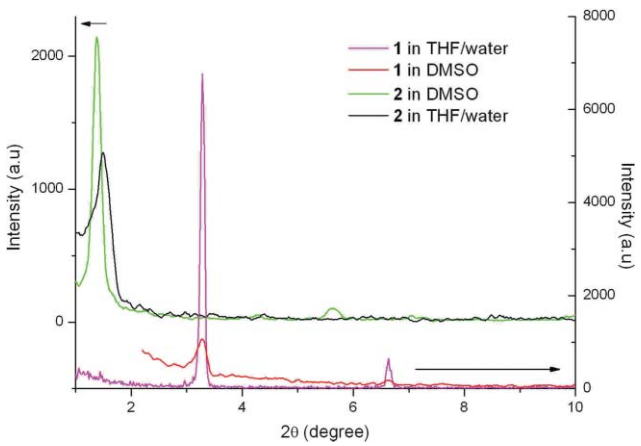


**Fig. 6** Small angle XRD patterns of xerogels of **1** and **2** in THF–water and DMSO.

 

peaks from THF–water are stronger and sharper than those from DMSO. So, the molecular array in THF–water is more ordered than that in DMSO. The good diffraction pattern for **2** in DMSO is characterized by four reflection peaks of 6.31, 3.15, 2.09 and 1.57 nm in the low angle region, which have a periodicity of 1/1, 1/2, 1/3 and 1/4. Apparently, a good lamellar organization within the aggregates of **2** in DMSO gel was formed with an interlayer distance of 6.31 nm,[13] which is longer than the period in the crystal state (5.26 nm). On the other hand, the intensity of the diffraction peaks of THF–water gel is weak and the lattice period shifts to 5.97 nm. Therefore, the solvent plays a crucial role in the molecular packing of **2** in the long range in the gel phase, which is different from gel systems of **1**.

**Molecular packing model.** As noted before, both compounds can self-assemble into 1-D ordered fibres, in which molecules are packed into J aggregates with the planarization of chromophores. To further clarify how the gelator molecules were arranged within the superstructure, the geometric optimization of gelators was firstly estimated by using AM1 force field, and then the optimized molecules were used to simulate the energy-minimized packing model by using the MM+ molecular mechanics force field (Hyperchem 8.0).[14] It is revealed that **1** has V-shaped configuration and its length is 3.3 nm in fully extended configuration, which is much longer than the long-range period (2.74 nm) obtained from the XRD measurement. After energy minimization, a linear molecular array with a sheet structure for **1** could be obtained, as shown in Fig. 7a, in which a tilted molecular arrangement could be observed and the aromatic moieties formed excellent head-to-tail stacking (J aggregate) with a intermolecular distance of 3.3 Å. However, the width of the sheet (*ca.* 3.0 nm) is still larger than 2.74 nm. There is a possibility that the sheets also adopt a tilted packing model in another stacking axis, as represented in Fig. 7b, because V-shaped configuration suppresses the parallel packing. In such a model, the long-range period is in accordance with the period obtained from XRD data.

Molecule **2** with the same extended molecular length as that of **1** also prefers to self-assemble along 1D direction. Because the lattice periods in THF–water and DMSO gels obtained from XRD investigations are much larger than the molecular length with the fully extended structure, the two kinds of the bimolecular lamellar is possible for molecule **2**, as shown in Fig. 5c and f. In the first packing model with the bimolecular layer (Fig. 7c), the length of the repeated unit is *ca.* 6.0 nm (Fig. 7e), being in agreement with the value of THF–water gel. If this bimolecular layer has a mismatch arrangement, as illustrated in Fig. 7d, the layer period is identical to that of crystal of **2** (Fig. 7d). In another possible bimolecular layer, two monomolecular sheets are arranged parallel to each other and it exhibits a long-range period of 6.3 nm (Fig. 7f and 7g). Therefore, molecule **2** may self-assemble into 1-D nanofibers with this bimolecular packing model in DMSO.

**Gelation-induced emission enhancement.** Based on the above discussions, it is known that **1** and **2** exhibit the aggregation-induced emission in crystal state, which may be induced by the formation of J aggregates and the planarization of the fluorophores. It inspires us to study the fluorescent properties of **1** and **2** in gel phases. Fig. 8 shows the time-dependent fluorescence spectra of **1** and **2** in THF–water and DMSO. It clearly shows that the hot solutions of **1** and **2** are weakly luminescent, while

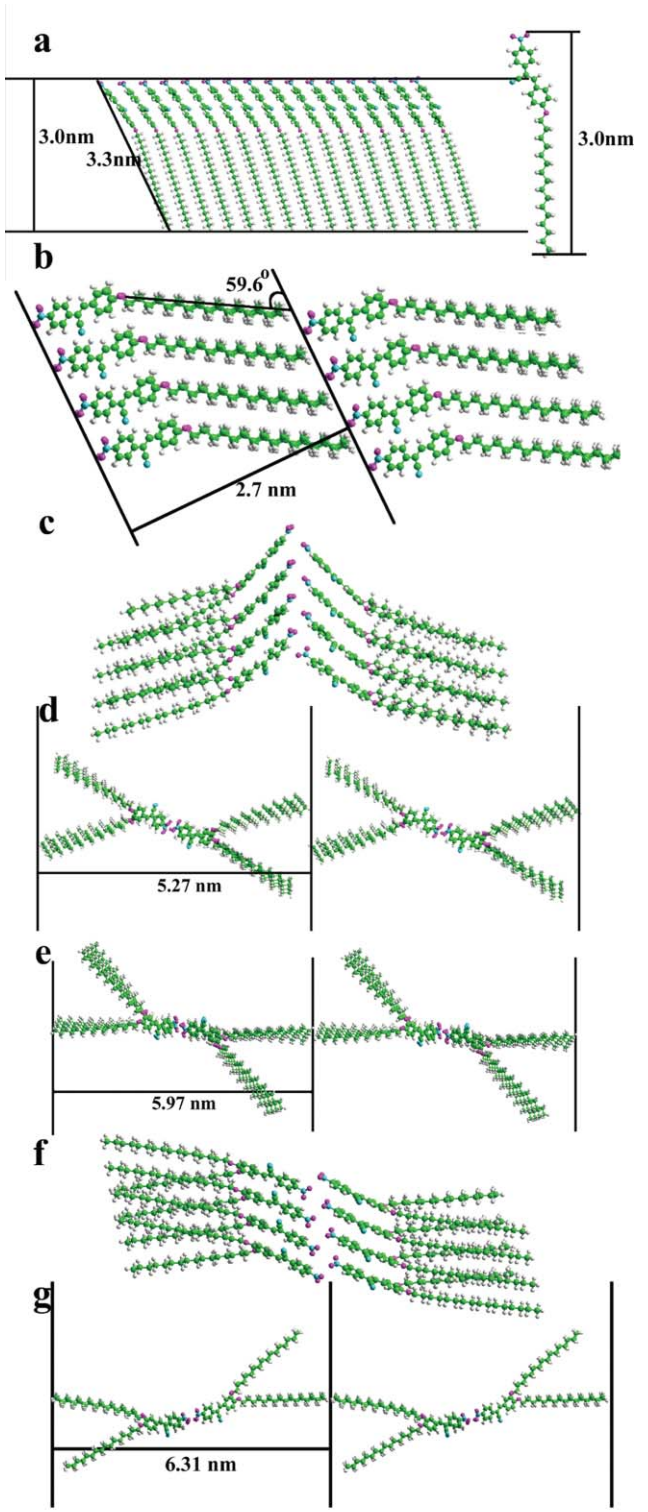


**Fig. 7** A schematic representation of molecular packing models of **1** in THF–water, DMSO and crystal state (a and b), and **2** in crystal state (c, d), THF–water (c, e) and DMSO (f and g).

their emissions are enhanced significantly with the temperature decreasing. For example, the photoluminescence spectrum of **1** in hot THF–water solution is nearly a flat line parallel to the abscissa (Fig. 8a). After cooling the hot solution for 1 min the

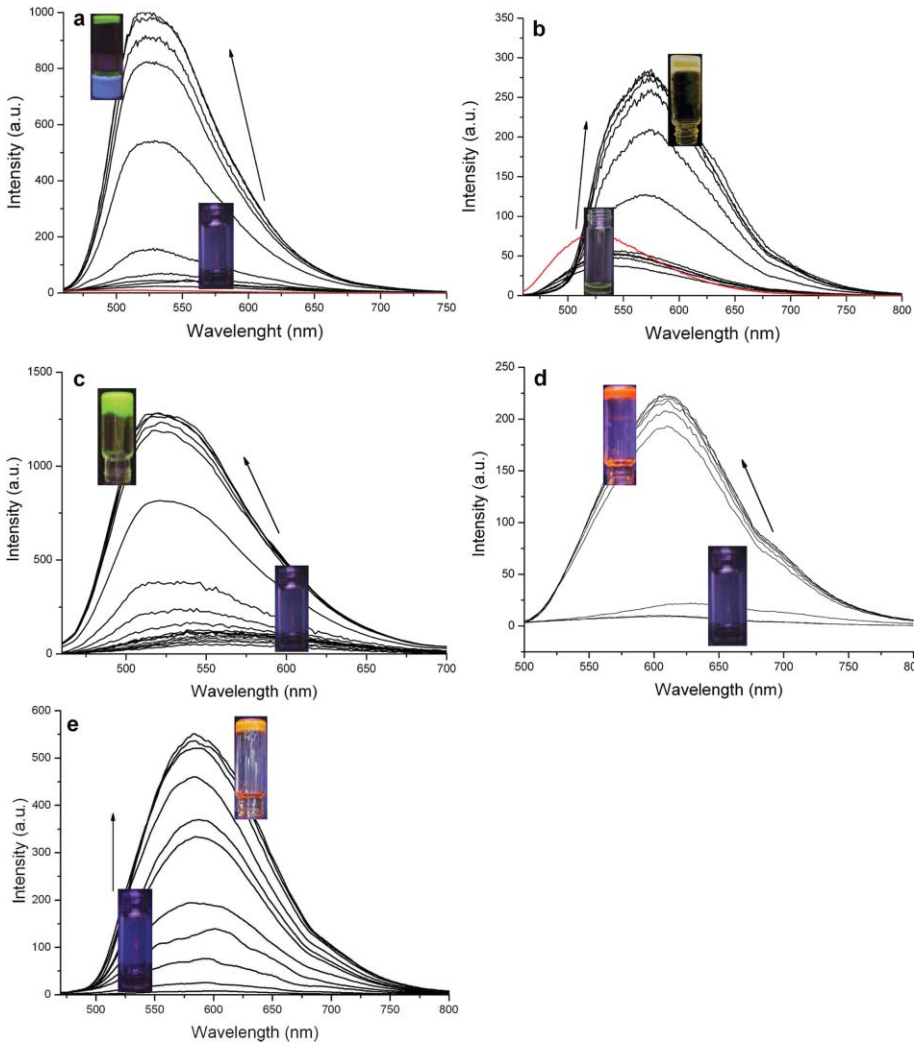


**Fig. 8** Time-dependent fluorescence spectra of **1** in THF–water (a) and DMSO (c), **2** in THF–water (b), DMSO (d) and acetone (e). Red lines are the fluorescence curves of **1** and **2** in THF solution. The concentrations of all samples are 0.1 wt/vol%. The samples in a and b firstly were heated to 60 °C and cooled to room temperature naturally. The samples in c and d firstly were heated to 100 °C. The testing interval time is 30 s.

emission at 535 nm increases slowly, afterwards, the emission intensity increases swiftly. After 5 min the gel is formed and the maximal peak blue-shifts to 525 nm, whose strength is 40-fold higher than that in the hot THF–water solution and *ca.* 90-fold higher than that of THF solution at the same concentration. In hot DMSO solution **1** gives one weak emission band at 550 nm, which gradually increases and also blue-shifts to 525 nm with 20-fold increase in the emission intensity. This suggests that the solvent polarity dose not affect the emission peak location and molecular packing of **1** in gel phases. Moreover, blue-shift of emission peaks may be induced by the disappearance of polar solvent effect because of the formation of large molecular aggregates, as shown in Fig. 3a and c.

Contrarily, the weak emission peak at 540 nm of **2** in hot THF–water solution red-shifted markedly to 574 nm accompanying with an enhancement of the emission when the sample was cooled down naturally for 3 min. After 13 min the system transferred into yellow gel phase with strong yellow fluorescence, whose intensity is 7-fold higher than that in the hot THF–water solution. On the other hand, the hot DMSO solution of **2** can be quickly gelatinized within 1 min. The maximal emission peak of **2** in hot DMSO solution is located at 608 nm, which slightly red-shifts to 610 nm in gel phase. The red-shift in emission spectra indicates the delocalization of the exciton across the self-assembled aggregates. Due to efficient exciton migration within the aggregates, emission occurs mainly from aggregates of lower energy resulting in a red shift in the wavelength.[15] Similarly, AIE is observed in DMSO gel of **2**, and its DMSO gel emits strong red fluorescence with 25-fold enhancement (Fig. 8d). Moreover, the gel phase formed by **2** in acetone also possesses excellent AIE characteristic with 70-fold enhancement and emits strong orange fluorescence (maximal peak at 584 nm). Therefore, the emitting color of **2** in gel phase and fluorescence enhanced degree can be controlled by the solvent.

Temperature-dependent fluorescence spectra of **1** and **2** in different solvent systems can tell us the fluorescent transition temperature. At a concentration of 0.1 wt/vol%, THF–water and DMSO gels of **1** have same transition temperature (40 °C), THF–water and acetone gels of **2** possess lower transition temperature (35 °C). However, DMSO gel of **2** show highest transition temperature and reach 60 °C (Fig. S6†). Thus, the

 

multicolor and temperature-sensitive fluorescent switches can be obtained.

## Conclusions

Two new D-π-A type organogelators **1** and **2** bearing one and two alkoxyl units, respectively, were synthesized. It is interesting that aggregation-induced emission can be realized in the gel phase. Moreover, the morphologies of assemblies and AIE activity can be controlled by the alkoxyl chain and solvent. In THF–water and DMSO gel systems, **1** shows the same packing model and the photophysical properties. Contrarily, the self-assembly and fluorescence characteristics of molecule **2** strongly depend on the solvent. Finally, the temperature-sensitive fluorescence switches with different emitted colors can be obtained by easily adjusting the type of the solvents and the number of the alkoxyl chains.

## Experimental Section

Instruments. Infrared spectra were recorded using a Nicolet-360 FTIR spectrometer by incorporating the samples into KBr disks. The UV–vis spectra were recorded on a Mapada UV-1800pc spectrophotometer. C, H, and N elemental analyses were performed on a Perkin-Elmer 240 C elemental analyzer. Photoluminescence measurements were taken on a Varian FLR006 luminescence spectrophotometer. X-ray Diffraction (XRD) patterns were determined on a Rigaku D/max-rA X-ray diffractometer with graphite-monochromatized Cu-Kα radiation ($\lambda = 1.5418$ Å). The accelerating voltage was set at 50 kV, with 100 mA fluxes at a scanning rate of 0.02° $S^{-1}$ in the 2 $\theta$ range of 1–10° and 0.05° $S^{-1}$ in the 2$\theta$ range of 10–40°. The XRD patterns of the xerogels were obtained by casting wet gel samples in a glass flask followed by the evaporation of the solvent naturally. Scanning electron microscope (SEM) observations were carried out on a Japan Hitachi model X-650 Scaning electron microscope. The samples for these measurements were prepared by casting little amounts of wet gels on silicon wafers and drying naturally, and then being coated by gold film. $^1$H and $^{13}$C NMR spectra were recorded on a Mercury Plus 500 MHz NMR.

### Synthetic procedures and characterizations

Molecules **1** and **2** could be easily obtained by the dehydration reaction of 4-(hexadecyloxy)benzaldehyde (**3**) and 3,4-bis(hexadecyloxy)benzaldehyde (**4**) with 4-nitrophenylacetonitrile, respectively, as shown in Scheme 1 and 2. **3** and **4** were obtained by previously described synthetic procedures.[16]

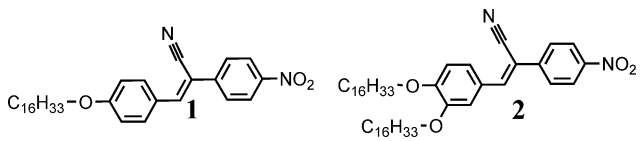


**Scheme 1** Molecular structures of **1** and **2**.

**(Z)-3-(4-(Hexadecyloxy)phenyl)-2-(4-nitrophenyl) acrylonitrile (1).** A solution of **3** (0.6 g, 1.7 mmol) and 4-nitrophenylacetonitrile (0.28 g, 1.7 mmol) in ethanol (20 mL) was heated to dissolve and then 0.1 mL of piperidine

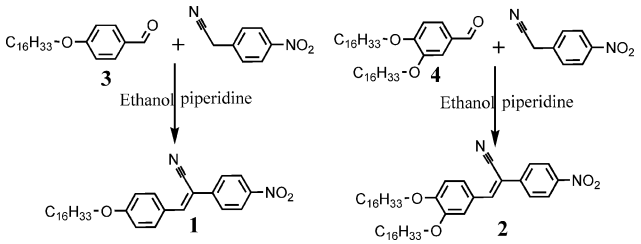


**Scheme 2** Synthesis route of **1** and **2**.

was added. After 2 h the solution was cooled down to room temperature and a large amounts of yellow solids were separated out from the solution. Pure product could be obtained by the vacuum filtration and washing with cooled ethanol. Yield 90.2%. mp 107–108 °C. $\nu_{max}$/cm$^{-1}$ 3070, 2961, 2917, 2850, 2213, 1580, 1508, 1471 and 1334. Element analysis (%): Calcd for $C_{31}H_{42}N_2O_3$, C, 75.88; H, 8.63; N, 5.71; Found: C, 75.80; H, 8.60; N, 5.68. $^1$H NMR (500 MHz, TMS, $CDCl_3$) $\delta$ 8.22 (d, $J$ = 8.5 Hz, 2 H), 7.61 (d, $J$ = 8.5 Hz, 2 H), 7.42 (s, 1 H), 7.07 (d, $J$ = 8.5 Hz, 2 H), 6.75 (d, $J$ = 8.5 Hz, 2 H), 3.94 (t, $J$ = 6.5 Hz, 2 H), 1.76 (m, 2 H), 1.42 (m, 2 H), 1.33–1.25 (m, 24 H), 0.88 (t, $J$ = 6.5 Hz, 3 H). $^{13}$C NMR (125 MHz, $CDCl_3$) $\delta$ 162.12, 147.51, 145.12, 141.20, 131.98, 126.32, 125.45, 124.34, 117.80, 115.14, 105.91, 68.41, 31.93, 29.68, 29.36, 29.09, 25.98, 22.70, 14.12.

**(Z)-3-(3,4-Bis(hexadecyloxy)phenyl)-2-(4-nitrophenyl)acrylonitrile (2).** **2** was synthesized by the same procedure of **1**. Yield 80.0%. mp 98–100 °C. $\nu_{max}$/cm$^{-1}$ 3046, 2955, 2918, 2849, 2211, 1578, 1514, 1466, 1441 and 1333. Element analysis (%): calcd for $C_{47}H_{74}N_2O_4$, C, 77.21; H, 10.20; N, 3.83; Found: C, 77.10; H, 10.18; N, 3.79. $^1$H NMR (500 MHz, TMS, $CDCl_3$): 8.23 (d, $J$ = 8.5 Hz, 2 H), 7.62 (d, $J$ = 8.5 Hz, 2 H), 7.41 (s, 1 H), 6.74 (m, 2 H), 6.57 (s, 1 H), 3.98 (t, $J$ = 6.5 Hz, 2 H), 3.64 (t, $J$ = 6.5 Hz, 2 H), 1.86 (m, 2 H), 1.80 (m, 2 H), 1.49 (m, 2 H), 1.44 (m, 2 H), 1.33–1.25 (m, 48 H), 0.88 (t, $J$ = 6.5 Hz, 6 H). $^{13}$C NMR (125 MHz, $CDCl_3$) $\delta$ 244.61, 244.56, 152.56, 149.16, 147.48, 145.47, 141.27, 126.31, 125.69, 125.45, 124.34, 117.93, 113.18, 112.62, 105.74, 69.33, 69.12, 31.94, 29.72, 29.39, 29.13, 29.05, 26.04, 22.70, 14.12

## Acknowledgements

This project was sponsored by the Scientific Research Foundation for the Returned Overseas Chinese Scholars, State Education Ministry, Open Project of the State Key Laboratory of Supramolecular Structure and Materials (SKLSSM200901), the National Natural Science Foundation of China (NNSFC 20874034), and the 973 Program (2009CB939701).

## Notes and references

1 (*a*) P. Terech and R. G. Weiss, *Chem. Rev.*, 1997, **97**, 3133; (*b*) D. J. Abdallah and R. G. Weiss, *Adv. Mater.*, 2000, **12**, 1237; (*c*) J. H. van Esch and B. L. Feringa, *Angew. Chem., Int. Ed.*, 2000, **39**, 2263; (*d*) L. A. Estroff and A. D. Hamilton, *Chem. Rev.*, 2004, **104**, 1201; (*e*) N. M. Sangeetha and U. Maitra, *Chem. Soc. Rev.*, 2005, **34**, 821; (*f*) A. R. Hirst and D. K. Smith, *Chem.–Eur. J.*, 2005, **11**, 5496; (*g*) A. Brizard, R. Oda and I. Huc, *Top. Curr. Chem.*, 2005, **256**, 167; (*h*) F. Fages, *Angew. Chem., Int. Ed.*, 2006, **45**, 1680; (*i*) M. George and R. G. Weiss, *Acc. Chem. Res.*, 2006, **39**, 489; (*j*) D. K. Smith, *Adv. Mater.*, 2006, **18**, 2773; (*k*) K. Sada, M. Takeuchi, N. Fujita, M. Numata and S. Shinkai, *Chem. Soc. Rev.*, 2007, **36**, 415; (*l*) A. Ajayaghosh and V. K. Praveen, *Acc. Chem. Res.*, 2007, **40**, 644; (*m*) Z. Yang and B. Xu, *J. Mater. Chem.*,

2007, **17**, 23; (*n*) A. R. Hirst, B. Escuder, J. F. Miravet and D. K. Smith, *Angew. Chem., Int. Ed.*, 2008, **47**, 8002; (*o*) M. M. Piepenbrock, G. O. Lloyd, N. Clarke and J. W. Steed, *Chem. Rev.*, 2010, **110**, 1960.

2 (*a*) X. C. Yang, R. Lu, P. C. Xue, B. Li, D. F. Xu, T. F. Xu and Y. Y. Zhao, *Langmuir*, 2008, **24**, 13730; (*b*) Z. Yang, G. Liang and B. Xu, *Acc. Chem. Res.*, 2008, **41**, 315; (*c*) Y. M. Zhang, Q. Lin, T. B. Wei, X. P. Qin and Y. Li, *Chem. Commun.*, 2009, 6074; (*d*) X. Wu, S. Ji, Y. Li, B. Li, X. Zhu, K. Hanabusa and Y. Yang, *J. Am. Chem. Soc.*, 2009, **131**, 5986; (*e*) A. Wicklein, S. Ghosh, M. Sommer, F. Würthner and M. Thelakkat, *ACS Nano*, 2009, **3**, 1107; (*f*) P. C. Xue, R. Lu, Y. Huang, M. Jin, C. H. Tan, C. H. Bao, Z. M. Wang and Y. Y. Zhao, *Langmuir*, 2004, **20**, 6470; (*g*) S. R. Haines and R. G. Harrison, *Chem. Commun.*, 2002, 2846; (*h*) A. Vintiloiu and J. C. Leroux, *J. Controlled Release*, 2008, **125**, 179; (*i*) Y. M. Zhang, Q. Lin, T. B. Wei, X. P. Qin and Y. Li, *Chem. Commun.*, 2009, 6074; (*j*) H. Jintoku, T. Sagawa, M. Takafuji and Hirotaka Ihara, *Org. Biomol. Chem.*, 2009, **7**, 2430.

3 (*a*) T. Kato, Y. Hirai, S. Nakaso and M. Moriyama, *Chem. Soc. Rev.*, 2007, **36**, 1857; (*b*) J. Liu, P. He, J. Yan, X. Fang, J. Peng, K. Liuand and Y. Fang, *Adv. Mater.*, 2008, **20**, 2508.

4 (*a*) J. D. Luo, Z. L. Xie, J. W. Y. Lam, L. Cheng, H. Y. Chen, C. F. Qiu, H. S. Kwok, X. W. Zhan, Y. Q. Liu, D. B. Zhu and B. Z. Tang, *Chem. Commun.*, 2001, 1740; (*b*) J. Seo, J. W. Chung, E. H. Jo and S. Y. Park, *Chem. Commun.*, 2008, 2794; (*c*) Y. Hong, J. W. Y. Tangand and B. Z. Lama, *Chem. Commun.*, 2009, 4332; (*d*) Y. P. Li, F. Z. Shen, H. Wang, F. He, Z. Q. Xie, H. Y. Zhang, Z. M. Wang, L. L. Liu, F. Li, M. Hanif, L. Ye and Y. G. Ma, *Chem. Mater.*, 2008, **20**, 7312; (*e*) S. Park, J. Seo, S. H. Kim and S. Y. Park, *Adv. Funct. Mater.*, 2008, **18**, 726; (*f*) J. Seo, J. W. Chung, E. H. Jo and S. Y. Park, *Chem. Commun.*, 2008, 2794; (*g*) J. W. Chung, B. K. An and S. Y. Park, *Chem. Mater.*, 2008, **20**, 6750.

5 (*a*) C. Y. Bao, R. Lu, M. Jin, P. C. Xue, C. H. Tan, G. F. Liu and Y. Y. Zhao, *Org. Biomol. Chem.*, 2005, **3**, 2508; (*b*) P. C. Xue, R. Lu, G. J. Chen, Y. Zhang, H. Nomoto, M. Takafuji and H. Ihara, *Chem.–Eur. J.*, 2007, **13**, 8231; (*c*) P. Chen, R. Lu, P. C. Xue, T. H. Xu, G. J. Chen and Y. Y. Zhao, *Langmuir*, 2009, **25**, 8395; (*d*) G. Palui and A. Banerjee, *J. Phys. Chem. B*, 2008, **112**, 10107; (*e*) Y. Hong, J. W. Y. Tang and B. Z. Lama, *Chem. Commun.*, 2009, 4332; (*f*) Y. L. Chen, Y. X. Lv, Y. Han, B. Zhu, F. Zhang, Z. S. Bo and C. Y. Liu, *Langmuir*, 2009, **25**, 8548; (*g*) T. H. Kim, D. G. Kim, M. Lee and T. S. Lee, *Tetrahedron*, 2010, **66**, 1667; (*h*) M. Wang, D. Zhang, G. Zhang and D. Zhu, *Chem. Phys. Lett.*, 2009, **475**, 64; (*i*) H. Wang, W. Zhang, X. Dong and Y. Yang, *Talanta*, 2009, **77**, 1864; (*j*) N. Yan, G. He, H. Zhang, L. Ding and Y. Fang, *Langmuir*, 2010, **26**, 5909.

6 C. Zhao, A. Wakamiya, Y. Inukai and S. Yamaguchi, *J. Am. Chem. Soc.*, 2006, **128**, 15934.

7 (*a*) F. Gao, T. Xie, Z. B. Cheng, N. Hu, L. Yang, Y. Gong, S. T. Zhang and H. J. Li, *J. Fluoresc.*, 2008, **18**, 787; (*b*) X. C. Yang, R. Lu, H. P. Zhou, P. C. Xue, F. Y. Wang, P. Chen and Y. Y. Zhao, *J. Colloid Interface Sci.*, 2009, **339**, 527.

8 A. Chowdhury, S. Wachsmann-Hogiu, P. R. Bangal, I. Raheem and L. A. Peteanu, *J. Phys. Chem. B*, 2001, **105**, 12196.

9 (*a*) B. An, S. Kwon, S. Jung and S. Y. Park, *J. Am. Chem. Soc.*, 2002, **124**, 14410; (*b*) Y. Li, F. Li, H. Zhang, Z. Xie, W. Xie, H. Xu, B. Li, F. Shen, L. Ye, M. Hanif, D. Ma and Y. Ma, *Chem. Commun.*, 2007, 231.

10 (*a*) P. C. Xue, R. Lu, D. M. Li, M. Jin, C. Y. Bao, Y. Y. Zhao and Z. M. Wang, *Chem. Mater.*, 2004, **16**, 3702; (*b*) T. Shimizu and M. Masuda, *J. Am. Chem. Soc.*, 1997, **119**, 2812.

11 (*a*) K. Jang, J. M. Kinyanjui, D. W. Hatchett and D. Lee, *Chem. Mater.*, 2009, **21**, 2070; (*b*) G. S. Lim, B. M. Jung, S. J. Lee, H. H. Song, C. Kim and J. Y. Chang, *Chem. Mater.*, 2007, **19**, 460.

12 (*a*) M. Masuda, V. Vill and T. Shimizu, *J. Am. Chem. Soc.*, 2000, **122**, 12327; (*b*) M. M. Rahman, M. Czaun, M. Takafuji and H. Ihara, *Chem.–Eur. J.*, 2008, **14**, 1312.

13 J. Liu, J. Yan, X. Yuan, K. Liu, J. Peng and Y. Fang, *J. Colloid Interface Sci.*, 2008, **318**, 397.

14 (*a*) F. Würthner, C. Thalacker, S. Diele and C. Tschierske, *Chem.–Eur. J.*, 2001, **7**, 2245; (*b*) L. E. Sinks, B. Rybtchinski, M. Limura, B. A. Jones, A. J. Goshe, X. Zuo, D. M. Tiede, X. Li and M. R. Wasielewski, *Chem. Mater.*, 2005, **17**, 6295; (*c*) P. C. Xue, R. Lu, X. C. Yang, L. Zhao, D. F. Xu, Y. Liu, H, Z. Zhang, H. Nomoto, M. Takafuji and H. Ihara, *Chem.–Eur. J.*, 2009, **15**, 9824.

15 (*a*) P. Jonkheijm, F. J. M. Hoeben, R. Kleppinger, J. van Herrikhuyzen, A. P. H. J. Schenning and E. W. Meijer, *J. Am. Chem. Soc.*, 2003, **125**, 15941; (*b*) K.-Y. Peng, S.-A. Chen and W.-S. Fann, *J. Am. Chem. Soc.*, 2001, **123**, 11388; (*c*) R. Varghese, S. J. George and A. Ajayaghosh, *Chem. Commun.*, 2005, 593; (*d*) S. J. George and A. Ajayaghosh, *Chem.–Eur. J.*, 2005, **11**, 3217.

16 (*a*) F. J. A. Hundscheid and J. B. F. N. Engberts, *J. Org. Chem.*, 1984, **49**, 3088; (*b*) T. Nakanishi, D. G. Kurth, Y. Shen, J. Wang, P. Fernandes, H. Moehwald, S. Yagai, M. Funahashi and T. Kato, *J. Am. Chem. Soc.*, 2008, **130**, 9236.



 